Article

Long-Term Planting of *Taxodium* Hybrid 'Zhongshanshan' Can Effectively Enhance the Soil Aggregate Stability in Saline–Alkali Coastal Areas

Xiaoshu Niu [1,2,†] , Xin Liu [1,2,†], Tao Li [3], Jie Lin [1], Shenghua Qin [4], Fulin Jing [4], Xiang Zhang [1], Jinchi Zhang [1,*] and Jiang Jiang [2,*]

[1] Jiangsu Province Key Laboratory of Soil and Water Conservation and Ecological Restoration, Nanjing Forestry University, 159 Longpan Road, Nanjing 210037, China; smalltreeniu@njfu.edu.cn (X.N.); liuxinswc@njfu.edu.cn (X.L.); jielin@njfu.edu.cn (J.L.); zzzxia@njfu.edu.cn (X.Z.)

[2] Co-Innovation Center for Sustainable Forestry in Southern China, Nanjing Forestry University, 159 Longpan Road, Nanjing 210037, China

[3] China Design Group, Nanjing 210014, China; wanglingswc@gmail.com

[4] Dafeng Forest Farm, Yancheng 224111, China; zhangwrswc@gmail.com (S.Q.); liuxinlixnly@gmail.com (F.J.)

* Correspondence: zhang8811@njfu.edu.cn (J.Z.); jiangjiang@njfu.edu.cn (J.J.)

† These authors contributed equally to this work.

Abstract: Not enough research has been conducted on the mechanisms influencing the stability of soil aggregates in coastal saline–alkaline soil and the dynamic changes in aggregates in the succession process of coastal saline–alkaline soil brought on by longer planting times. In this study, soil aggregate composition, stability, and influencing factors of 0–20 cm, 20–40 cm, and 40–60 cm soil layers in different planting time stages were analyzed in the reclaimed land at the initial stage of afforestation and the *Taxodium* hybrid 'Zhongshanshan' plantation with planting times of 6, 10, 17, and 21 years. The results show that, with the increase in planting time, the aggregate stability of the plantation increased significantly. In the 0–20 cm soil layer, the geometric mean diameter (GMD) and aggregate size >0.25 mm ($R_{0.25}$) increased by 81.15% and 89.80%, respectively, when the planting time was 21 years, compared with the reclaimed land. The structural equation (SEM) showed that planting time had a direct positive effect (path coefficient 0.315) on aggregate stability. However, soil sucrase (0.407) and β-glucosidase (0.229) indirectly improved the stability of aggregates by affecting soil organic carbon. In summary, the establishment of *Taxodium* hybrid 'Zhongshanshan' plants on coastal saline–alkali land is beneficial for stabilizing soil aggregates, improving soil structure, and boosting soil quality. Long-term planting of *Taxodium* hybrid 'Zhongshanshan' can be an effective measure for ecological restoration in this region.

Keywords: planting time; coastal saline–alkali land; stability of soil aggregates; *Taxodium* hybrid 'Zhongshanshan'; soil enzyme activity

1. Introduction

Excessive sodium and other salt ions in the coastal saline–alkali land cause soil binding agents to disperse and colloidal ion composition to change, which in turn causes soil aggregates to disintegrate, soil structure to deteriorate, soil quality to decline, and vegetation coverage to decrease [1,2]. In the context of global warming, saline–alkali land is an important potential reserve land resource, and the construction of forestry ecological engineering based on tree planting is very important for the restoration of vegetation in saline–alkali land, improving soil quality, increasing soil carbon storage, improving the ecosystem, and helping to realize the "double carbon target". Improving saline–alkaline land through plant planting is a crucial step [3]. Studies have shown that phytoremediation can significantly reduce soil salt content and improve soil physicochemical properties [4,5]. Soil properties have a critical impact on ecosystem restoration [6]. One of the key indicators to assess the quality

of the soil is aggregate stability. Soil aggregate is the fundamental building block of soil structure and a significant component of soil [7,8]. Thus, changes in aggregate stability can be used to infer changes in soil quality, and soil aggregates themselves can be employed as a critical indication of ecosystem restoration [9,10]. Enzyme activity, aggregate structure, and physical and chemical characteristics of soil react quickly to variations in the surrounding environment during the establishment of forestry ecosystems [11]. When ecosystems are restored, there is typically a gradual rise in soil organic matter as well as a rise in biological variety and populations, which influences aggregate changes [12]. To improve soil quality, it is crucial to investigate how plantation aggregate changes at different planting dates.

One of the key elements of plantation ecosystems is planting time, which can have an impact on the stability and composition of soil aggregates by affecting the decomposition of litter [13], carbon storage and flux [14], microbial activity and community character [15], and other factors. According to earlier research, when vegetation is restored in regions affected by soil erosion, the porosity of the soil aggregate is greatly increased, and the aggregate structure is clearly stable [16]. The stability of soil aggregates gradually rose as the number of restoration years increased, as did the macroaggregates [17]. Soil aggregates were significantly impacted by restoration duration and soil depth during the process of vegetation restoration, and following vegetation restoration, soil's ability to sequester carbon was increased [18]. In karst regions, reforestation greatly enhances the conservation of soil organic carbon by fostering the development of soil macroaggregates [19]. Organic carbon can also encase itself by promoting the formation of aggregates, forming a physical barrier that reduces its decomposition by soil enzymes [20]. Soil aggregates and organic carbon have a strong link. Organic carbon participates in the formation of aggregates through organic and inorganic cementation, and the development and formation of aggregates is also an important mechanism of organic carbon fixation. Soil enzymes affect the transformation and accumulation of organic matter and the decomposition of humus in soil, and then cause the change in aggregates [21,22]. Thus, it is worthwhile to investigate the connection between enzyme activity and soil aggregate stability.

However, previous studies on aggregates have focused more on the organic carbon and nitrogen content of aggregates [23], the effects of agricultural practices [24,25], the effects of organic fertilizer application [26], the effects of different land uses [20,27], the relationship with microbial diversity [28], the effects of adding biological carbon [29–31], etc. Few research has been conducted on how the timing of planting affects aggregate stability. Studies on the stability of aggregates mainly focus on the tropical and subtropical secondary forest in Parana [32], the subtropical red soil region in South China [33], the degraded grassland region in Hebei Province [34], and the black soil region in Northeast China [35]. However, studies on the coastal saline–alkali land are very rare. Considering that *Taxodium* hybrid 'Zhongshanshan' has excellent characteristics of flood resistance, waterlogging tolerance [36], and salt tolerance [37], and can actively improve soil properties and soil quality [38], it is suitable for afforestation in saline–alkali coastal land. So, the goal of this study was to examine the stability and composition of soil aggregates under *Taxodium* hybrid 'Zhongshanshan' at different planting times in coastal saline–alkali land, analyze the relationship between environmental factors, enzyme activity, and aggregate stability, and identify the mechanisms that influence soil aggregate stability.

Based on previous studies, we put forward the following hypotheses: (1) the construction of *Taxodium* hybrid 'Zhongshanshan' plantations can reduce the effect of salinization in the soil; (2) soil enzyme activity indirectly affects the stability of aggregates; and (3) the stability of soil aggregates in coastal saline–alkali land increase with the increase in planting time.

2. Materials and Methods

2.1. General Situation of the Study Area and Plot Setting

At the intersection of the North Subtropical Zone and the Warm Temperate Zone, Yancheng City, Jiangsu Province, China's Dafeng District (33°05′ N, 120°49′ E) features an

obvious monsoon environment, prevailing southeasterly and easterly winds in the spring, high wind speeds, and frequent typhoons in the summer. The yearly average temperature is 14.1 °C. The hottest month is July, with an average temperature of 27.0 °C, while January is the coldest, with an average temperature of 0.8 °C. There is 1068.0 mm of yearly rainfall and 1361.0 mm of annual evaporation on average. The study area is a silt beach formed under the accumulation of sediment, which is a typical wetland of the Yellow Sea beach. The soil type belongs to the coastal silt soil, where the proportion of silt is high, and the soil fertility is low. The overall salt composition is mainly sulfate, and the original soil conductivity is roughly 1600–5000 μS/cm [39].

The effect of planting time on soil aggregate was studied by using the method of space for time. Based on our investigation, a sample plot survey method was adopted in April 2023. In Dafeng Forest Farm, Yancheng City, Jiangsu Province, China (Figure S1), the 6-, 10-, 17-, and 21-year *Taxodium* hybrid 'Zhongshanshan' artificial forest with a relatively high proportion in this area was selected as the research object (hereinafter referred to as TZ_6, TZ_{10}, TZ_{17}, and TZ_{21}), and the reclaimed land at the early stage of afforestation was selected as the control group (hereinafter referred to as CK). Reclaimed land has evolved from tidal flats. In the early stages of the development and utilization of tidal flats, it is necessary to reduce groundwater through land preparation and ditching. The reclaimed land before afforestation is usually contracted to local residents to grow soybeans, rapeseeds and other crops. Three 20 m × 20 m fixed plots were randomly distributed for the four kinds of Zhongshan fir forests and the reclamation land at the initial stage of afforestation, with a total of 15 plots. These plots essentially had the same habitat conditions.

2.2. Soil Sample Collection

Among the 20 × 20 m standard quadrates, 3 small quadrates of 1 m × 1 m were randomly selected according to an "S" shape. The undisturbed soil samples were collected from the three soil layers of 0–20, 20–40, and 40–60 cm of each small quadrate in the form of soil blocks. The fresh soil samples of the same soil layer collected from three different quadrates in the same place were mixed evenly and immediately put into the foam box with an ice pack. Following the removal of the stones and plant remnants in the laboratory, some of the soil was immediately placed in a refrigerator set at −4 °C, while the remainder was allowed to air dry for subsequent operations. At the same time, a soil profile of 1 m in length, 0.5 m in width, and 1 m in depth was set in the center of each sample plot. Three soil layers of 0–20, 20–40, and 40–60 cm were selected from top to bottom with a ring knife to collect undisturbed soil samples. A total of 90 soil samples were taken in the laboratory for the following measurements.

2.3. Determination of Physical and Chemical Properties of Soil

The pH and conductivity of soil were measured using the potential method (ratio of soil to water, 5:1). The exchangeable cations were determined via the sodium acetate method, the exchangeable Na^+ content was determined using the ammonium acetate–ammonium hydroxide method, and the alkalization degree was calculated using the ratio of exchangeable Na^+ content to exchangeable cation content [40]. The determination of soil moisture was performed by the drying method [41]. Soil bulk density, non-capillary porosity, capillary porosity, total porosity, soil permeability, and drainage capacity were measured by the ring knife method (V, 100 cm^3) [41]. Soil organic carbon (SOC) was determined by the external heating method with potassium dichromate [42]. Soil microbial biomass carbon (MBC) was determined by chloroform fumigation extraction [43]. The content of nitrate nitrogen was determined by ultraviolet colorimetry [44]. The content of ammonium nitrogen was determined by indophenol blue colorimetry [44].

2.4. Soil Aggregate Classification and Stability Evaluation

(1) Classification of soil aggregate particle group samples: The international soil particle classification standard was used to divide the soil aggregate particle group (the

U.S. Department of Agriculture Soil particle Grading Standards roughly divided the soil aggregate into 4 groups according to particle size, which were <0.053 mm, 0.053–0.25 mm, 0.25–2 mm, and >2 mm), separated and slightly modified according to Stemmer et al. [45]. A total of 50.0 g of fresh soil sample was weighed and placed in a beaker filled with 250 mL of distilled water (water-to-water ratio, 5:1). The solution was soaked overnight. Ultrasonic dispersion was conducted with a probe-type ultrasonic generator (JYD-650, Shanghai Zhixin Instrument Co., Ltd., Shanghai, China, 2001) at low energy (170 J/min) for 5 min. The particle groups with 2000–200 μm particle sizes were separated via the wet sieve method, and then the particle groups with 200–20 μm particle sizes were separated by the sedimentation siphon method, and then the particle groups with 20–2 μm and <2 μm particle sizes were separated by the centrifugal method. After freeze-drying of the obtained particle group sample, the particle group with 2000–200 μm particle sizes was passed through a 100-mesh sieve and set aside.

(2) The mean meight diameter (MWD) and geometric mean diameter (GMD) of soil aggregates were calculated by Equations (1) and (2), respectively. The content of stable aggregates >0.25 mm ($R_{0.25}$) was calculated by Equation (3). The fractal dimension (D) is obtained by taking the logarithm base 10 on both sides of Equation (4) to obtain Equation (5).

$$MWD = \frac{\sum\limits_{i=1}^{n} (R_i W_i)}{\sum\limits_{i=1}^{n} W_i} \tag{1}$$

$$GMD = \exp\left[\frac{\sum\limits_{i=1}^{n} W_i \ln R_i}{\sum\limits_{i=1}^{n} W_i}\right] \tag{2}$$

$$R_{0.25} = \frac{M_{r>0.25}}{M_T} \times 100\% \tag{3}$$

$$\frac{M(r < R_i)}{M_T} = \left(\frac{R_i}{R_{max}}\right)^{(3-D)} \tag{4}$$

$$lg\left[\frac{M(r < R_i)}{M_T}\right] = (3-D)lg\left(\frac{R_i}{R_{max}}\right) \tag{5}$$

where R_i is the average diameter (mm) of water-stable aggregates of each particle size; W_i is the mass percentage (%) of water-stable aggregates of each particle grade. $M_{r>0.25}$ is the mass of water-stable aggregates with particle size >0.25 mm; M_T is the total mass of water-stable aggregates; $M_{(r<Ri)}$ is the mass of aggregates with particle size less than R_i. R_{max} is the maximum particle size of aggregates.

2.5. Determination of Soil Enzyme Activity

According to German et al., the activities of soil peroxidase (POD) and polyphenol oxidase (PHE) were analyzed [46]. Soil urease activity (URE) was determined by the sodium phenol–sodium hypochlorite colorimetric method [47]. Soil sucrase activity (SUC) was determined by 3, 5-dinitrosalicylic acid colorimetry with an absorbance of 508 nm [48]. Soil β–glucosidase activity (BG) was determined by fluorescence microplate analysis [49].

2.6. Data Analysis

The data were statistically analyzed using Excel 2021 software, and the results were presented as mean ± standard deviation. The variations in soil physicochemical parameters, enzyme activities, and aggregate stability in various planting times and soil layers were compared using one-way ANOVA (SPSS, version 26.0, Chicago, IL, USA). The effects of planting time and soil depth on each indicator were investigated using a two-way ANOVA (SPSS, version 26.0, Chicago, IL, USA). The impact of physicochemical characteristics on

enzyme activity was investigated using Canoco5 (Microcomputer Power, Ithac, NY, USA) redundancy analysis (RDA). Using the genescloud platform (https://www.genescloud.cn), Spearman correlation analysis was carried out on the soil aggregate stability, physicochemical characteristics, and enzyme activity. A correlation calorific value map was created. The structural equation model (SEM) linking physical and chemical characteristics of soil, enzyme activity, and aggregate stability was created using IBM SPSS Amos 25 GrapHics software (Amos, version 25.0, Chicago, IL, USA). Origin 2018 software was used for drawing (Origin, 2018 version, Northampton, MA, USA).

3. Results

3.1. Physical and Chemical Properties of Soil

Planting time and soil depth significantly affected soil physicochemical properties (Figures 1 and 2). The lengthening planting period brought about a notable rise in soil bulk density (Figure 1e), whereas soil pH decreased (Figure 2b). Ammonium nitrogen, nitrate nitrogen, and microbial biomass carbon all decreased first and then increased (Figure 2d,e,g), and the soil organic carbon fluctuated (Figure 2f). Compared with the three soil layers in group CK, the average conductivity and basicity of TZ_{21} decreased significantly by 69.89% and 36.56%, respectively (Figure 2a,c). In the 0–20 cm soil layer, ammonium nitrogen in TZ_{21} increased by 53.97% (Figure 2d) compared to the CK group, while microbial biomass carbon increased by 21.99% (Figure 2g). As the soil layer deepens, nitrate nitrogen, soil organic carbon, and microbial biomass carbon showed a downward trend (Figure 2e–g), while soil pH and basicity showed an upward trend (Figure 2b,c). The basicity of TZ_{21} in the 40–60 cm soil layer increased by 398.33% compared with the 0–20 cm soil layer (Figure 2c), and the soil organic carbon in TZ_6 decreased by 84.19% (Figure 2f).
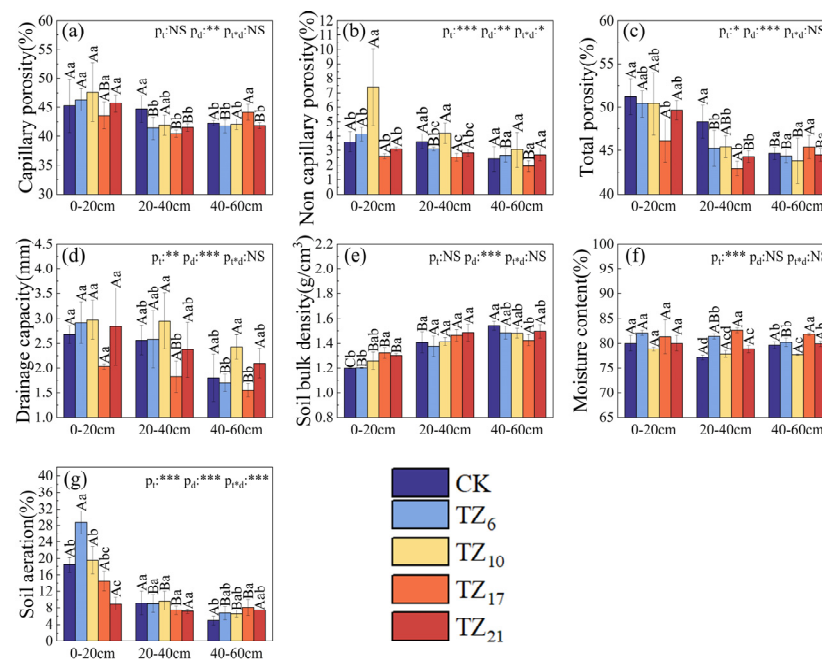

Figure 1. Soil physical properties. (**a**): Capillary porosity; (**b**): Non capillary porosity; (**c**): Total porosity; (**d**): Drainage capacity; (**e**): Soil bulk density; (**f**): Moisture content; (**g**): Soil aeration. Although distinct capital letters signify notable differences between soil layers at the same planting time, distinct lowercase letters suggest notable variations between planting intervals within the same soil layer ($p < 0.05$). p_t represents planting time, p_d represents soil depth, ***: $p < 0.001$, **: $p < 0.01$, *: $p < 0.05$, and NS indicates no significant difference. CK: reclaimed land, TZ_6: planting time of 6 years, TZ_{10}: planting time of 10 years, TZ_{17}: planting time of 17 years, TZ_{21}: planting time of 21 years.
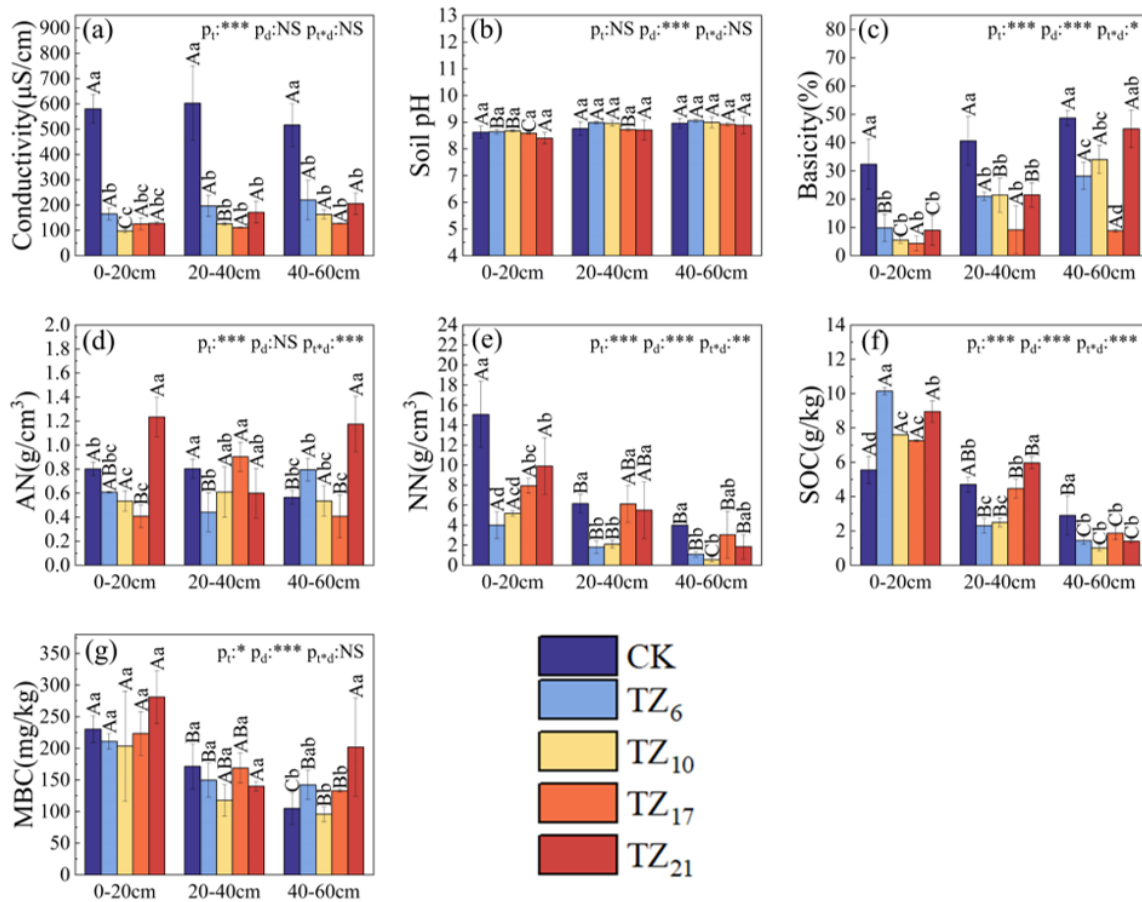
Figure 2. Soil chemical properties. (**a**): Conductivity; (**b**): Soil pH; (**c**): Basicity; (**d**): Ammonium nitrogen; (**e**): nitrate nitrogen; (**f**): Soil organic carbon; (**g**): Microbial biomass carbon. Although distinct capital letters signify notable differences between soil layers at the same planting time, distinct lowercase letters suggest notable variations between planting intervals within the same soil layer ($p < 0.05$). p_t represents planting time, p_d represents soil depth, ***: $p < 0.001$, **: $p < 0.01$, *: $p < 0.05$, and NS indicates no significant difference. SOC: soil organic carbon, AN: ammonium nitrogen, MBC: microbial biomass carbon, NN: nitrate nitrogen. CK: reclaimed land, TZ_6: planting time of 6 years, TZ_{10}: planting time of 10 years, TZ_{17}: planting time of 17 years, TZ_{21}: planting time of 21 years.

3.2. Analysis of Soil Enzyme Activity

Figure 3 shows the changes in different enzyme activities with planting time and soil depth. With the increase in planting time, the activities of urease, polyphenol oxidase, and peroxidase first increased and then decreased (Figure 3b–d), while β-glucoside activity fluctuated (Figure 3e). In the 0–20 cm soil layer, urease activity in TZ_{17} increased by 59.47% compared with the CK group (Figure 3b). Peroxidase activity in TZ_6 increased by 33.92% compared with the CK group (Figure 3d). The deeper the soil layer, the more pronounced the decreasing trend observed in the activities of urease, β-glucoside, and sucrase (Figure 3a,b,e); the activity of polyphenol oxidase showed an upward trend Figure 3c), and the activity of peroxidase showed fluctuations (Figure 3d). The soil layer of 40–60 cm was higher than that of 0–20 cm. CK-TZ_{21} sucrase activity decreased by 93.16%, 94.74%, 99.55%, 80.66%, and 99.04%, respectively (Figure 3a).
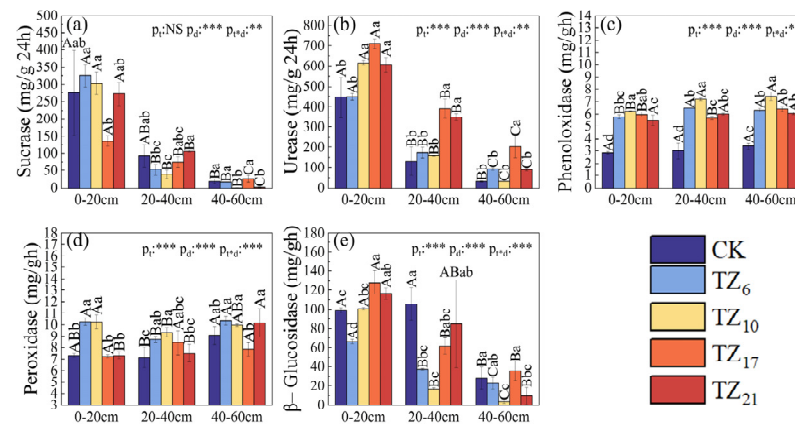
Figure 3. Soil enzyme activity. (**a**): Sucrase activity; (**b**): Urease activity; (**c**): Phenoloxidase activity; (**d**): Peroxidase activity (**e**): β–Glucosidase activity. Although distinct capital letters signify notable differences between soil layers at the same planting time, distinct lowercase letters suggest notable variations between planting intervals within the same soil layer ($p < 0.05$). pt represents planting time, pd represents soil depth, ***: $p < 0.001$, **: $p < 0.01$, *: $p < 0.05$, and NS indicates no significant difference. CK: reclaimed land, TZ_6: planting time of 6 years, TZ_{10}: planting time of 10 years, TZ_{17}: planting time of 17 years, TZ_{21}: planting time of 21 years.

3.3. Soil Water Stability Aggregate Size Content Characteristics

The distribution characteristics of aggregates in the study area showed that aggregates with a diameter of <0.25 mm (micro-aggregates) accounted for the majority, with an average content of 77.68% (Figure 4). The percentage of large aggregates (aggregates with a diameter of >0.25 mm) in the 0–20 cm soil layer increased as planting time increased. The percentage of aggregates with a dimension of 0.053 mm–0.25 substantially fell by 47.05% when compared to the CK group, while the percentage of big aggregates increased by 89.96% (Table 1). Large aggregate content initially declined and subsequently increased between 20 and 40 cm of soil (Figure 4). At the same planting period, there was a notable decline in the percentage of large aggregates as the soil layer became deeper, while the percentage of aggregates with a diameter of less than 0.053 mm experienced a considerable increase. For instance, the percentage of large aggregates in the TZ_{21} group's 40–60 cm soil layer dropped by 93.75% as compared to between 20 and 40 cm of soil, while the percentage of aggregates with a diameter of less than 0.053 mm increased by 213.99% (Table 1).
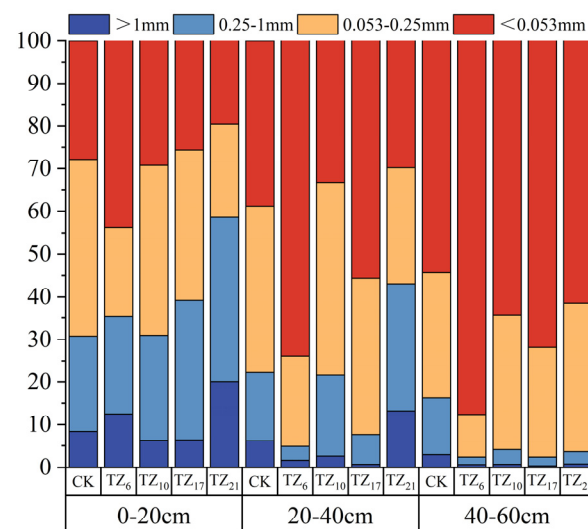
Figure 4. Composition of soil aggregates. CK: reclaimed land, TZ_6: planting time of 6 years, TZ_{10}: planting time of 10 years, TZ_{17}: planting time of 17 years, TZ_{21}: planting time of 21 years.

Table 1. Size class of soil aggregates.

Soil Layer	Soil Aggregate Fraction	CK	TZ$_6$	TZ$_{10}$	TZ$_{17}$	TZ$_{21}$
0–20 cm	>1 mm	0.084 ± 0.009 Ac	0.125 ± 0.009 Ab	0.063 ± 0.005 Ad	0.063 ± 0.005 Ad	0.2 ± 0.132 Aa
	0.25–1 mm	0.225 ± 0.021 Ac	0.228 ± 0.014 Ac	0.248 ± 0.009 Ac	0.329 ± 0.006 Ab	0.385 ± 0.007 Aa
	0.053–0.25 mm	0.413 ± 0.011 Aa	0.21 ± 0.005 Ac	0.397 ± 0.019 Ba	0.352 ± 0.024 Bb	0.219 ± 0.006 Cc
	<0.053 mm	0.279 ± 0.008 Cbc	0.438 ± 0.015 Ca	0.293 ± 0.025 Bb	0.256 ± 0.022 Cc	0.196 ± 0.005 Cd
20–40 cm	>1 mm	0.061 ± 0.002 Bb	0.017 ± 0.004 Bd	0.026 ± 0.005 Bc	0.007 ± 0.001 Be	0.132 ± 0.004 Ba
	0.25–1 mm	0.161 ± 0.015 Bc	0.032 ± 0.006 Be	0.19 ± 0.022 Bb	0.069 ± 0.005 Bd	0.299 ± 0.013 Ba
	0.053–0.25 mm	0.39 ± 0.016 Ab	0.213 ± 0.025 Ad	0.452 ± 0.009 Aa	0.367 ± 0.003 Ab	0.271 ± 0.011 Bc
	<0.053 mm	0.388 ± 0.003 Bc	0.739 ± 0.033 Ba	0.332 ± 0.023 Bd	0.556 ± 0.007 Bb	0.298 ± 0.018 Bd
40–60 cm	>1 mm	0.03 ± 0.003 Ca	0.007 ± 0.001 Bbc	0.007 ± 0.003 Cbc	0.004 ± 0.001 Bc	0.008 ± 0.002 Cb
	0.25–1 mm	0.132 ± 0.011 Ba	0.017 ± 0.006 Bc	0.034 ± 0.006 Cb	0.02 ± 0.001 Cc	0.028 ± 0.003 Cbc
	0.053–0.25 mm	0.295 ± 0.02 Bb	0.1 ± 0.013 Bd	0.314 ± 0.01 Cb	0.258 ± 0.009 Cc	0.349 ± 0.014 Aa
	<0.053 mm	0.544 ± 0.029 Ad	0.876 ± 0.018 Aa	0.644 ± 0.016 Ac	0.718 ± 0.01 Ab	0.615 ± 0.015 Ac

Data represent the average of three replicates ± standard errors. Although distinct capital letters signify notable differences between soil layers at the same planting time, distinct lowercase letters suggest notable variations between planting intervals within the same soil layer ($p < 0.05$). CK: reclaimed land, TZ$_6$: planting time of 6 years, TZ$_{10}$: planting time of 10 years, TZ$_{17}$: planting time of 17 years, TZ$_{21}$: planting time of 21 years.

3.4. Stability Analysis of Soil Aggregates

With the increase in planting time, MWD, GMD, and R$_{0.25}$ showed a significant upward trend, while fractional dimension showed a significant downward trend (Figure 5a–d). As the soil depth increased, MWD, GMD, and R$_{0.25}$ showed a decreasing trend, while fractional dimension showed an increasing trend (Figure 5a–d). The MWD of soil layers TZ$_{21}$ that were 0–20 cm and 20–40 cm increased by 66.77% and 60.94% (Figure 5a), GMD grew by 81.15% and 61.28% (Figure 5b), and R$_{0.25}$ increased by 89.80% and 93.88% (Figure 5c) in comparison to the control group. Fractional dimension decreased by 8.39% and 4.81%, respectively (Figure 5d). Compared with the 0–20 cm soil layer in the TZ$_{21}$ group, MWD, GMD, and R$_{0.25}$ decreased by 80.65%, 78.7%, and 93.7%, respectively, and fractional dimension increased by 14.67% in the 40–60 cm soil layer (Figure 5a–d).
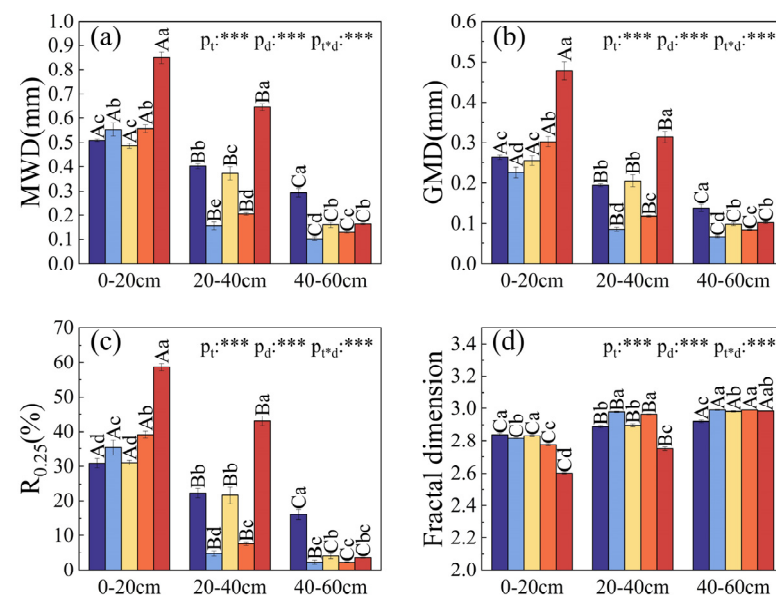

Figure 5. Stability indicators of soil aggregates at different planting times and soil depths. (**a**): Mean weight diameter; (**b**): Geometric mean diameter; (**c**): Content of stable aggregates >0.25 mm; (**d**): Fractal dimension. Diverse lowercase letters denote significant differences between planting periods in the same soil layer ($p < 0.05$), whereas different capital letters show significant variations between soil layers with the same planting time. pt represents planting time, pd represents soil depth, ***: $p < 0.001$, NS indicates no significant difference. CK: reclaimed land, TZ$_6$: planting time of 6 years, TZ$_{10}$: planting time of 10 years, TZ$_{17}$: planting time of 17 years, TZ$_{21}$: planting time of 21 years.

3.5. Impact of the Physical and Chemical Characteristics of Soil on the Activity of Enzymes

Soil physicochemical properties and soil enzyme activity were subjected to redundancy analysis (RDA). The findings indicated a negative correlation between urease activity and the activities of peroxidase, polyphenol oxidase, and β-glucosidase. Sucrase activity revealed an inverse relationship with soil bulk density, basicity, and pH and a positive correlation with soil aeration, moisture content, drainage capacity, soil organic carbon, microbial biomass carbon, total porosity, capillary porosity, nitrate nitrogen, and electrical conductivity. Soil enzyme activity was mostly influenced by environmental factors, with total porosity being the dominant explanatory variable, accounting for 47.2% ($p < 0.01$) of the variation in enzyme activity. Soil physical and chemical parameters had a noteworthy effect on soil enzyme activities, as evidenced by the cumulative explanatory variation of the first and second axes, which was 96.86% (Figure 6).
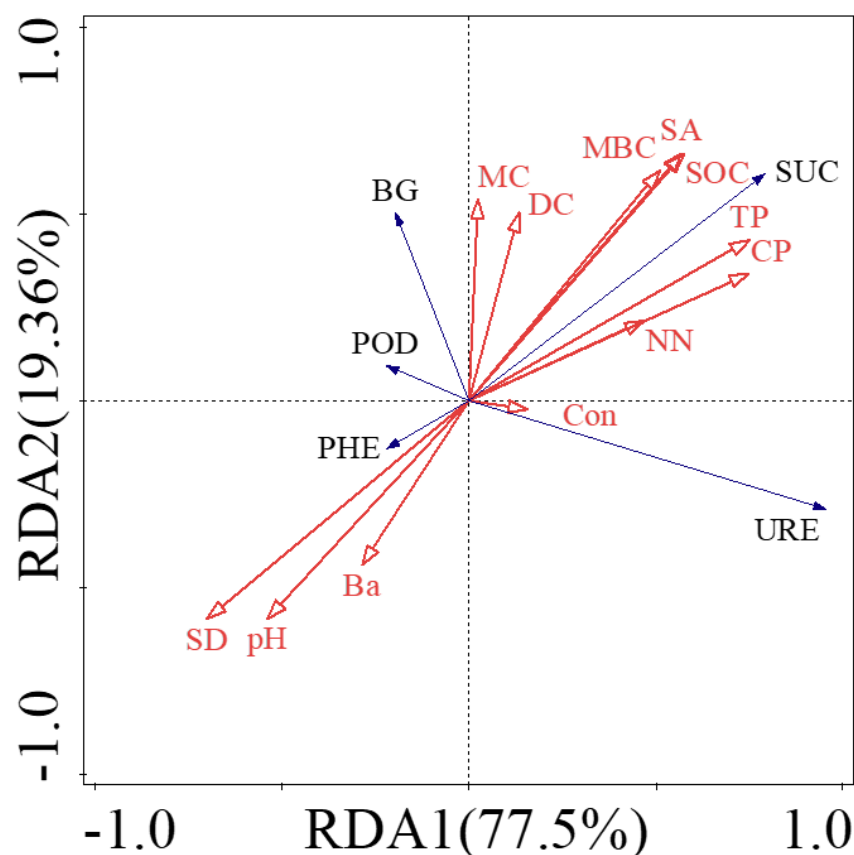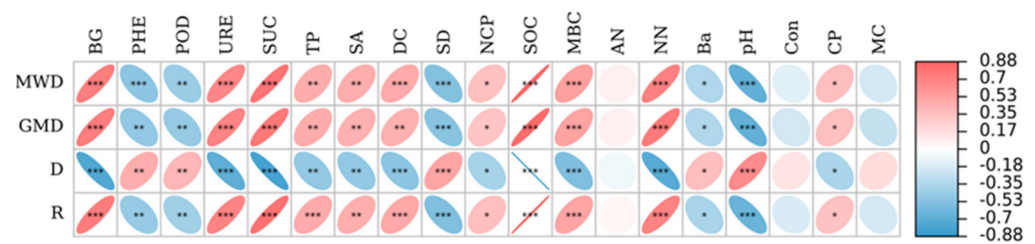

Figure 6. Redundancy analysis of soil physicochemical properties and enzyme activity. BG: β−Glucosidase activity, POD: peroxidase activity, PHE: polyphenol oxidase activity, URE: urease activity, SUC: sucrase activity, AN: ammonium nitrogen, NN: nitrate nitrogen, Ba: basicity, Con: conductivity, CP: capillary porosity, TP: total porosity, MC: moisture content, DC: drainage capacity, SD: soil bulk density, SA: soil aeration.

3.6. Enzyme Activity and Soil Physicochemical Characteristics' Effects on Aggregate Stability

Spearman correlation analysis was performed on soil aggregate stability, enzyme activity, and other physicochemical properties to obtain the correlation calorific value map. The findings demonstrated a strong positive association ($p < 0.01$) between MWD, GMD, and $R_{0.25}$ and β-glucosidase activity, sucrase activity, urease activity, total porosity, soil aeration, soil organic carbon, nitrate nitrogen, drainage capacity, and microbial biomass carbon. Additionally, there was a significant positive correlation ($p < 0.05$) between MWD, GMD, and $R_{0.25}$ and non-capillary and capillary porosity. While there was a strong negative association ($p < 0.05$) with basicity and a substantial negative association ($p < 0.01$) with

polyphenol oxidase activity, peroxidase activity, soil bulk density, and soil pH, there was no significant link with ammonium nitrogen, conductivity, or moisture content (Figure 7).

Figure 7. Heat map of correlation between soil aggregate stability, enzyme activity, and other soil physicochemical properties. *: $p < 0.05$, **: $p < 0.01$,***: $p < 0.001$. R: $R_{0.25}$, BG: β−Glucosidase activity, POD: peroxidase activity, PHE: polyphenol oxidase activity, URE: urease activity, SUC: sucrase activity, AN: ammonium nitrogen, NN: nitrate nitrogen, Ba: basicity, Con: conductivity, CP: capillary porosity, NCP: non-capillary porosity, TP: total porosity, MC: moisture content, DC: drainage capacity, MBC: microbial biomass carbon, SD: soil bulk density, SA: soil aeration, SOC: soil organic carbon.

3.7. Mechanism of Aggregate Stability Impacts of Soil Physical and Chemical Characteristics, Enzyme Activity, and Planting Time

Seven indices were found to have a strong and significant correlation with aggregate stability through Spearman analysis. GMD, an index that measures aggregate stability, was used to construct the structural equation (SEM) that connects soil physical and chemical properties, enzyme activity, aggregate stability, and planting time. The results showed that the planting time had a positive effect on the stability of aggregates directly (path coefficient was 0.315, Figure 8a), and the planting time also had an indirect effect on the stability of aggregates. The direct effects of soil enzyme activities on the stability of aggregates were small and insignificant, and soil enzyme activities mainly improved the stability of aggregates through indirect effects (Figure 8a). For example, the activities of sucrase and β-glucosidase improved the stability of aggregates by directly affecting soil organic carbon (path coefficients were 0.407 and 0.229, respectively, Figure 8a,b). By positively impacting the amount of nitrate nitrogen in aggregates, urease indirectly increased their stability (path coefficient was 0.479, Figure 8a,b). Soil pH had a negative effect on enzyme activity and thus on aggregate stability (path coefficient was −0.405, Figure 8a,b).
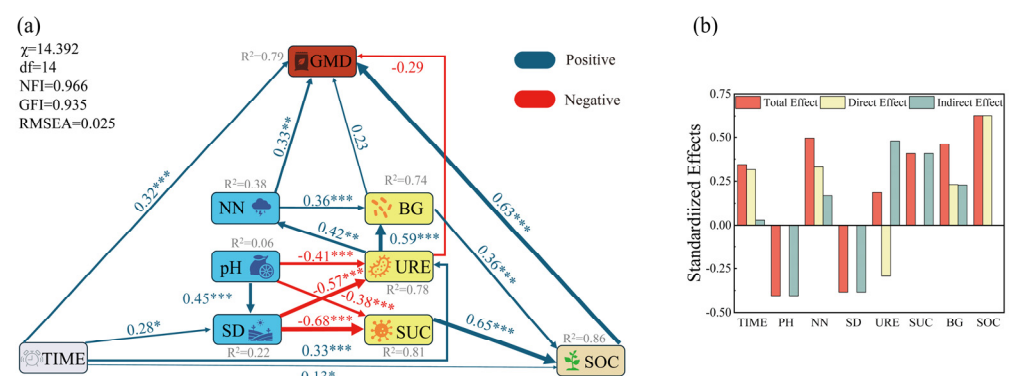
Figure 8. (**a**) A structural equation model that illustrates the direct and indirect effects of soil physicochemical characteristics, enzyme activity, and planting time on soil aggregate stability. (**b**) This subfigure indicates how planting time, soil physicochemical characteristics, and enzyme activity affect aggregate stability directly, indirectly, and overall. ***: $p < 0.001$, **: $p < 0.01$, *: $p < 0.05$. The directional influence of one variable on another is shown by arrows. The standardized path coefficient is indicated by the numbers next to each arrow. Positive and negative correlations are shown by the blue and red arrows, respectively. BG: β−Glucosidase activity, URE: urease activity, SUC: sucrase activity, NN: nitrate nitrogen, SD: soil bulk density, SOC: soil organic carbon, TIME: planting time.

4. Discussion

4.1. Differences in Soil Physical and Chemical Properties with Planting Time and Soil Depth in Coastal Saline–Alkali Land

Soil aggregates disintegrate, soil structure deteriorates, and soil quality declines as a result of the excess sodium, potassium, and other salt ions present in the coastal saline–alkali soil, dispersing soil binding agents and changing the composition of colloidal ions [2]. Compared with bare soil, the salt content can be reduced by planting vegetation [50]. The results of this study showed that, compared with the control group, the conductivity and basicity of the forest land decreased significantly (Figure 2a,c), and soil pH also decreased gradually with the increase in planting time but did not reach a significant level (Figure 2b), indicating that soil ion content decreased significantly through the planting of the *Taxodium* hybrid 'Zhongshanshan', and soil conditions were continuously improved. The results are the same as those of the Yellow River Delta coastal saline–alkali land [51]. With the increase in soil layer, the basicity (Figure 2c) and soil bulk density (Figure 1e) of forest land significantly increased, while the contents of capillary porosity, soil ventilation (Figure 1a,g), nitrate nitrogen, soil organic carbon, and microbial biomass carbon (Figure 2e,f,g) significantly decreased, indicating that the improvement ability of planting *Taxodium* hybrid 'Zhongshanshan' on soil quality and structure decreased with the increase in soil layer. This is in line with several studies' conclusions [52–55]. In the 0–20 cm soil layer, nitrate nitrogen increased with the increase in planting time, while ammonium nitrogen first decreased and then increased (Figure 2d,e). This may be because changes in soil structure and properties affected soil mineralization characteristics with the increase in planting time. SOC changes in different soil layers were more complex (Figure 2f). SOC in the control group (0–20 cm) soil layer was much smaller than that of forest land, indicating that the soil organic carbon content was greatly increased after afforestation, which was consistent with the results of the research conducted in mangrove forests [56]. The reason is that after afforestation, a large amount of litter is produced, which makes organic carbon sources rich [57]. With the increase in planting time, SOC decreased first and then increased, which was the same as the conclusion of Deng et al.'s work [58].The possible reason is that after the construction of *Taxodium* hybrid 'Zhongshanshan' forest, a large amount of organic carbon accumulates on the soil surface at an early stage, but the rapid growth of *Taxodium* hybrid 'Zhongshanshan' requires a large amount of nutrients for its growth. Later, due to the increase in stand cover and the improvement of ground litter, water, and light conditions, soil respiration was weakened, and SOC content on the surface was restored. At the early stage of the 20–40 cm soil layer, soil carbon decreased, and then carbon storage gradually recovered to the level of reclamation land in the early stage of afforestation, and then net carbon income increased. This is the same as previous experiments in some areas [58–60]. The reason may be that although SOC content in surface soil is greatly increased after planting *Taxodium* hybrid 'Zhongshanshan' forest, SOC can only penetrate deep soil with water and other media [61,62]. Therefore, compared with surface soil, SOC content in deep soil will lag. With the gradual improvement of forest ecology, organic carbon will be continuously imported. SOC gradually increased, and eventually TZ_{21} surpassed CK. It is possible that the *Taxodium* hybrid's well-developed roots had an intercepting impact on the organic matter that migrated to the lower layer, trapping the nutrients primarily in the 0–40 cm soil layer, explaining the significantly greater SOC content in the 40–60 cm soil layer of the control group compared to the forest land. Consequently, the forest land's 40–60 cm soil layer had a much lower SOC level than the control group. The surface MBC content decreased first and then increased with the increase in planting time but did not reach a significant level (Figure 2g). The reason may be that the ecosystem was not stable in the early stages of afforestation, which led to a downward trend in microbial biomass carbon. After that, the amount of surface litter under the forest increased year by year, the environment was constantly improved, the microbial activity was improved, and the decomposed organic matter was enhanced. Therefore, the soil microbial biomass content increased year by year after more than 10 years of planting. Because of a drop in oxygen content, root exudates,

and plant and animal wastes in the soil, the MBC content drastically reduced as soil depth increased, causing deep soil to have a significantly lower MBC content than surface soil [63]. The change in MBC with time and soil depth is the same as that of secondary vegetation succession in semi-arid abandoned land on the Loess Plateau [64].

4.2. Analysis and Influencing Factors of Soil Enzyme Activity in Different Planting Times in Saline–Alkali Coastal Land

Planting time has an important effect on soil enzyme activity. Stand structure, forest microclimate, and plant and animal secretions change with increasing planting time, which directly or indirectly affects soil enzyme activity [65]. The activities of sucrase, urease, and β-glucosidase decreased with increasing soil depth (Figure 3a,b,e), consistent with the results of experiments conducted in coniferous forests in northern Finland [66]. This is caused by the soil surface plants' high nutritional content, high root density, copious root secretions, and sufficient litter supply, all of which support the growth and reproduction of both plants and animals as well as the release of associated enzymes [63]. But deep soil differs greatly from surface soil in terms of its physical and chemical characteristics, and the bulk density of the soil rises with the increase in soil depth (Figure 1e). Lower soil enzyme activity is found in lower soil layers due to plant root development inhibition and the reduced activity of soil microbes [67]. In particular, the activities of polyphenol oxidase and peroxidase, which are related to the decomposition of difficult-to-degrade carbon, did not decrease significantly with the increase in soil depth [68] (Figure 3c,d), which is comparable with the findings of the Northern Chinese Scots pine investigation [69]. The reason for the relatively small effect of oxidase activity on soil depth may be that the litter of the Chinese fir plantation is mainly composed of lignin, polyfiber, and polyphenols, which are difficult to decompose and have more chances to penetrate into the deep soil with water and other substances. Although they were substantially greater than those of the control group, the activities of peroxidase and polyphenol oxidase showed a declining trend as planting time increased (Figure 3c,d). It is probable that following afforestation, the amount of organic matter in the soil has decreased since microbes need to break down tough organic matter to obtain nutrients. After the improvement of the understory ecosystem, the nutrients provided by easily decomposed organic matter can meet the needs of microorganisms. At the same time, the microorganisms that produce polyphenol oxidase have poor competitive ability, and the enzyme activity for difficult-to-decompose organic matter will gradually decrease [70,71]. In addition, in this study, nitrate nitrogen showed an increasing trend with the increase in planting time (Figure 2e), and some studies showed that with the addition of N in larch forest land, β-glucosidase activity increased while polyphenol oxidase activity decreased, which was similar to the results of this experiment [70]. As the planting time increased, the activities of urease in the 0–40 cm soil layer initially grew and then dropped (Figure 3b), which was in line with the findings of Wu et al. [72]. However, Wang et al.'s study showed that urease decreased first and then increased with planting time [73], possibly due to different site conditions, climate, and other conditions. Redundancy analysis revealed that the explanation for soil enzyme activity was 47.2% and that there was a substantial correlation between soil enzyme activity and total porosity. It shows that increasing soil porosity has a positive effect on soil enzyme activity in saline–alkali land areas.

4.3. Analysis and Influencing Mechanism of Soil Aggregate Stability at Different Planting Times in Saline–Alkali Coastal Land

In this study, it was found that soil aggregates in group CK were mainly micro-aggregates, while the average content in the control group was 76.92% (Table 1). The soil structure was obviously improved after afforestation, which was consistent with previous studies [74,75]. The amount of macroaggregates in the 0–20 cm soil layer increased as planting time increased (Figure 4), and the proportion of TZ_{21} macroaggregates was close to 60%, indicating that the soil aggregate structure continued to improve with the increase in planting time. In North Chinese plantations, the content of soil macroaggregates first grew and subsequently dropped as planting times increased [23]. Planting *eucalyptus*

continuously made the soil aggregates less stable [76]. The inconsistent tree species, uneven soil, and widely varied planting time spans under investigation could all be contributing factors to the study's inconsistent findings. The soil aggregate's MWD, GMD, and $R_{0.25}$ all significantly decreased while the soil layer deepened, which was consistent with Le Bissonnais' study findings [77], indicating that soil layer depth significantly affected the stability of aggregates. As planting time increased, MWD, GMD, and $R_{0.25}$ of the 0–20 cm soil layer showed a growing pattern (Figure 5a–c), which was consistent with studies on vegetation restoration upon the conversion of cropland into forest on the Loess Plateau [16], showing that as planting times increased, soil aggregate stability improved over time. The change trend of 20–60 cm was the same, and all of them were W-shaped. The first potential explanation is that soil disturbance following afforestation operations causes a significant loss of deep soil organic carbon, which in turn causes a deterioration in soil stability [59,78,79]. Therefore, the stability of TZ_6 is significantly decreased compared with CK. Second, there are fewer litters in the reclaimed land in the early stage of afforestation. Furthermore, the *Taxodium* hybrid 'Zhongshanshan' is a fast-growing species that, in the early stages of its rapid growth, has a high demand for soil nutrients. Moreover, the pace at which litters decompose is faster than the rate at which they are produced. The instability of nutrient supply and demand leads to drastic changes in soil organic matter, resulting in fluctuations in aggregate stability [23]. Third, there were differences in the amount of litter, plant roots, microbiological activity, and canopy density during different growth and development stages, which could have an impact on aggregate stability. Aggregate stability dramatically declined in the 40–60 cm soil layer, which was in line with Kurmi et al.'s research findings [80]. The possible reason was that the roots of the *Taxodium* hybrid 'Zhongshanshan' were mostly distributed in the surface layer and had a certain blocking effect on the migration of organic matter to the lower layer. Consequently, when the soil layer grew deeper, the stability of forest aggregates dropped significantly.

Additionally, it was demonstrated using Spearman analysis, the SEM structural equation model, and other ecological statistical analysis techniques that planting time positively impacted aggregate stability and that afforestation enhanced soil quality and structure. The planting time impacted both directly and indirectly on aggregate stability; the latter was impacted by changes in the soil's chemical and physical characteristics [81] as well as enzyme activity [15,82]. Soil enzyme activity has a negligible and direct effect on aggregate stability; it mostly enhances aggregate stability indirectly by raising the amount of organic carbon in the soil. Furthermore, this confirms that soil organic carbon and aggregate stability have a direct positive link [49]. Among them, urease can also promote the improvement of aggregate stability by increasing the content of nitrate nitrogen. According to a report by Le et al., aggregate stability and soil nitrogen concentration are positively correlated [77]. Enzyme activity was negatively impacted by soil bulk density and pH [83–85], which lessened the impact of enzyme activity on aggregate stability. Thus, it is important to monitor changes in soil bulk density and pH during the afforestation of saline–alkali land, and it is important to remember that early afforestation may be susceptible to nitrogen limitation [86]. Therefore, the introduction of green fertilizer crops can be considered to better improve soil quality [87].

5. Conclusions

The dynamic changes in soil aggregate stability and the mechanisms controlling them at different planting periods of the *Taxodium* hybrid 'Zhongshanshan' were examined in this study. We discovered that after afforestation, the soil's conductivity and basicity dramatically dropped, significantly reducing the negative influence of soil salinization. Significantly inversely connected with soil bulk density and pH, soil aggregate stability had a positive correlation with β-glucosidase activity, urease activity, sucrase activity, soil organic carbon, nitrate nitrogen, and microbial biomass carbon. In coastal saline–alkaline land, nitrate nitrogen and organic carbon have a major influence on aggregate stability; the activity of enzymes indirectly influences aggregate stability. The stability of the soil

aggregate grew greatly as the planting time increased, and the large aggregate (>0.25 mm) showed an increasing tendency. The findings demonstrated that the establishment of a *Taxodium* hybrid 'Zhongshanshan' plantation may considerably improve the soil structure and quality of the saline–alkali coastal area.

References

1. Muhammad, K.; Dan, W.; Xie, K.; Lu, Y.; Shi, C.; Sabagh, A.E.; Gu, W.; Xu, P. Pre-sowing seed treatment with kinetin and calcium mitigates salt induced inhibition of seed germination and seedling growth of choysum (*Brassica rapa* var. *parachinensis). Ecotoxicol. Environ. Saf.* **2021**, *227*, 112921.

2. Xie, W.; Chen, Q.; Wu, L.; Yang, H.; Xu, J.; Zhang, Y. Coastal saline soil aggregate formation and salt distribution are affected by straw and nitrogen application: A 4-year field study. *Soil Tillage Res.* **2020**, *198*, 104535. [CrossRef]

3. Panta, S.; Flowers, T.; Lane, P.; Doyle, R.; Haros, G.; Shabala, S. Halophyte agriculture: Success stories. *Environ. Exp. Bot.* **2014**, *107*, 71–83. [CrossRef]

4. Nadal-Romero, E.; Cammeraat, E.; Pérez-Cardiel, E.; Lasanta, T. Effects of secondary succession and afforestation practices on soil properties after cropland abandonment in humid Mediterranean mountain areas. *Agric. Ecosyst. Environ.* **2016**, *228*, 91–100. [CrossRef]

5. Shao, T.; Gu, X.; Zhu, T.; Pan, X.; Zhu, Y.; Long, X.; Shao, H.; Liu, M.; Rengel, Z. Industrial crop *Jerusalem artichoke* restored coastal saline soil quality by reducing salt and increasing diversity of bacterial community. *Appl. Soil Ecol.* **2019**, *138*, 195–206. [CrossRef]

6. Toktar, M.; Papa, G.L.; Kozybayeva, F.E.; Dazzi, C. Ecological restoration in contaminated soils of Kokdzhon phosphate mining area (Zhambyl region, Kazakhstan). *Ecol. Eng.* **2016**, *86*, 1–4. [CrossRef]

7. Blanco-Canqui, H.; Lal, R. Mechanisms of Carbon Sequestration in Soil Aggregates. *Crit. Rev. Plant Sci.* **2004**, *23*, 481–504. [CrossRef]

8. Wu, T.; Schoenau, J.J.; Li, F.; Qian, P.; Malhi, S.S.; Shi, Y. Effect of tillage and rotation on organic carbon forms of chernozemic soils in Saskatchewan. *J. Plant Nutr. Soil Sci.* **2003**, *166*, 328–335. [CrossRef]

9. Ma, L.; Wang, Q.; Shen, S.T.; Li, F.C.; Li, L. Heterogeneity of soil structure and fertility during desertification of alpine grassland in northwest Sichuan. *Ecosphere* **2020**, *11*, e03161. [CrossRef]

10. Xiao, L.; Yao, K.; Li, P.; Liu, Y.; Chang, E.; Zhang, Y.; Zhu, T. Increased soil aggregate stability is strongly correlated with root and soil properties along a gradient of secondary succession on the Loess Plateau. *Ecol. Eng.* **2020**, *143*, 105671. [CrossRef]

11. Paz-Ferreiro, J.; Fu, S. Biological Indices for Soil Quality Evaluation: Perspectives and Limitations. *Land Degrad. Dev.* **2016**, *27*, 14–25. [CrossRef]

12. Feng, C.; Ma, Y.; Fu, S.; Chen, H.Y.H. Soil Carbon and Nutrient Dynamics Following Cessation of Anthropogenic Disturbances in Degraded Subtropical Forests. *Land Degrad. Dev.* **2017**, *28*, 2457–2467. [CrossRef]

13. Yunchao, L.; Lixin, C.; Wenbiao, D.; Yongan, B.; Xiaolan, L. Effects of Litter Decomposition on Soil N in *Picea mongolica* Forest at Different Forest Ages. *Forests* **2022**, *13*, 520. [CrossRef]

14. Xu, L.; Shi, Y.; Fang, H.; Zhou, G.; Xu, X.; Zhou, Y.; Tao, J.; Ji, B.; Xu, J.; Li, C.; et al. Vegetation carbon stocks driven by canopy density and forest age in subtropical forest ecosystems. *Sci. Total Environ.* **2018**, *631-632*, 619–626. [CrossRef] [PubMed]

15. Lucas-Borja, M.E.; de Santiago, J.H.; Yang, Y.; Shen, Y.; Candel-Pérez, D. Nutrient, metal contents and microbiological properties of litter and soil along a tree age gradient in Mediterranean forest ecosystems. *Sci. Total Environ.* **2019**, *650*, 749–758. [CrossRef] [PubMed]

16. Wang, Y.; Ran, L.; Fang, N.; Shi, Z. Aggregate stability and associated organic carbon and nitrogen as affected by soil erosion and vegetation rehabilitation on the Loess Plateau. *Catena* **2018**, *167*, 257–265. [CrossRef]
17. Yang, Y.F.; Wei, H.; Lin, L.W.; Deng, Y.S.; Duan, X.Q. Effect of Vegetation Restoration on Soil Humus and Aggregate Stability within the Karst Region of Southwest China. *Forests* **2024**, *15*, 292. [CrossRef]
18. Bai, Y.; Zhou, Y.; He, H. Effects of rehabilitation through afforestation on soil aggregate stability and aggregate-associated carbon after forest fires in subtropical China. *Geoderma* **2020**, *376*, 114548. [CrossRef]
19. Lan, J.C.; Long, Q.X.; Huang, M.Z.; Jiang, Y.X.; Hu, N. Afforestation-induced large macroaggregate formation promotes soil organic carbon accumulation in degraded karst area. *For. Ecol. Manag.* **2022**, *505*, 119884. [CrossRef]
20. Liu, M.; Han, G.L.; Zhang, Q. Effects of agricultural abandonment on soil aggregation, soil organic carbon storage and stabilization: Results from observation in a small karst catchment, Southwest China. *Agric. Ecosyst. Environ.* **2020**, *288*, 106719. [CrossRef]
21. Wang, J.J.; Shu, K.L.; Wang, S.Y.; Zhang, C.; Feng, Y.C.; Gao, M.; Li, Z.H.; Cai, H.G. Soil Enzyme Activities Affect SOC and TN in Aggregate Fractions in Sodic-Alkali Soils, Northeast of China. *Agronomy* **2022**, *12*, 2549. [CrossRef]
22. Wang, S.S.; Wang, Z.Q.; Fan, B.; Mao, X.H.; Luo, H.; Jiang, F.Y.; Liang, C.F.; Chen, J.H.; Qin, H.; Xu, Q.F.; et al. Litter Inputs Control the Pattern of Soil Aggregate-Associated Organic Carbon and Enzyme Activities in Three Typical Subtropical Forests. *Forests.* **2022**, *13*, 1210. [CrossRef]
23. Ma, Y.; Cheng, X.Q.; Kang, F.F.; Han, H.R. Dynamic characteristics of soil aggregate stability and related carbon and nitrogen pools at different developmental stages of plantations in northern China. *J. Environ. Manag.* **2022**, *316*, 115283. [CrossRef] [PubMed]
24. Zhang, L.; Su, X.; Meng, H.; Wang, H.; Yan, X.; Qin, D.; Liu, C.; Men, Y.; Zhang, X.; Song, X.; et al. Long-term cotton stubble return and subsoiling improve soil organic carbon by changing the stability and organic carbon of soil aggregates in coastal saline fields. *Soil Tillage Res.* **2024**, *241*, 106127. [CrossRef]
25. Yongxiang, G.; Haojie, F.; Min, Z.; Yuqing, S.; Jiaqi, W.; Yanli, L.; Chengliang, L. Straw returning combined with controlled-release nitrogen fertilizer affected organic carbon storage and crop yield by changing humic acid composition and aggregate distribution. *J. Clean. Prod.* **2023**, *415*, 137783.
26. Tian, S.Y.; Zhu, B.J.; Yin, R.; Wang, M.W.; Jiang, Y.J.; Zhang, C.Z.; Li, D.M.; Chen, X.Y.; Kardol, P.; Liu, M.Q. Organic fertilization promotes crop productivity through changes in soil aggregation. *Soil Biol. Biochem.* **2022**, *165*, 108533. [CrossRef]
27. Zhao, J.S.; Chen, S.; Hu, R.G.; Li, Y.Y. Aggregate stability and size distribution of red soils under different land uses integrally regulated by soil organic matter, and iron and aluminum oxides. *Soil Tillage Res.* **2017**, *167*, 73–79. [CrossRef]
28. Han, S.; Delgado-Baquerizo, M.; Luo, X.S.; Liu, Y.R.; Van Nostrand, J.D.; Chen, W.L.; Zhou, J.Z.; Huang, Q.Y. Soil aggregate size-dependent relationships between microbial functional diversity and multifunctionality. *Soil Biol. Biochem.* **2021**, *154*, 108143. [CrossRef]
29. Burrell, L.D.; Zehetner, F.; Rampazzo, N.; Wimmer, B.; Soja, G. Long-term effects of biochar on soil physical properties. *Geoderma* **2016**, *282*, 96–102. [CrossRef]
30. Zhang, Q.Q.; Song, Y.F.; Wu, Z.; Yan, X.Y.; Gunina, A.; Kuzyakov, Y.; Xiong, Z.Q. Effects of six-year biochar amendment on soil aggregation, crop growth, and nitrogen and phosphorus use efficiencies in a rice-wheat rotation. *J. Clean. Prod.* **2020**, *242*, 118435. [CrossRef]
31. Sun, F.F.; Lu, S.G. Biochars improve aggregate stability, water retention, and pore- space properties of clayey soil. *J. Plant Nutr. Soil Sci.* **2014**, *177*, 26–33. [CrossRef]
32. Thomaz, E.L.; Araujo-Junior, C.F.; Vendrame, P.R.; de Melo, T.R. Mechanisms of aggregate breakdown in (sub) tropical soils: Effects of the hierarchical resistance. *Catena* **2022**, *216*, 106377. [CrossRef]
33. Tang, X.; Qiu, J.C.; Xu, Y.Q.; Li, J.H.; Chen, J.H.; Li, B.; Lu, Y. Responses of soil aggregate stability to organic C and total N as controlled by land-use type in a region of south China affected by sheet erosion. *Catena* **2022**, *218*, 106543. [CrossRef]
34. Cheng, R.; Kesi, L.; Pengpeng, D.; Xinqing, S.; Dingyuan, Z.; Kaili, W.; Xiqiang, L.; Jiahuan, L.; Kun, W. Soil Nutrients Drive Microbial Changes to Alter Surface Soil Aggregate Stability in Typical Grasslands. *J. Soil Sci. Plant Nutr.* **2022**, *22*, 4943–4959.
35. Zhang, C.; Zhao, X.; Liang, A.J.; Li, Y.Y.; Li, X.Y.; Li, D.P.; Hou, N. Insight into the soil aggregate-mediated restoration mechanism of degraded black soil via biochar addition: Emphasizing the driving role of core microbial communities and nutrient cycling. *Environ. Res.* **2023**, *228*, 115895. [CrossRef] [PubMed]
36. Xuan, L.; Hua, J.F.; Zhang, F.; Wang, Z.Q.; Pei, X.X.; Yang, Y.; Yin, Y.L.; Creech, D.L. Identification and Functional Analysis of *ThADH1* and *ThADH4* Genes Involved in Tolerance to Waterlogging Stress in *Taxodium* hybrid 'Zhongshanshan 406'. *Genes* **2021**, *12*, 225. [CrossRef] [PubMed]
37. Zhou, L.J.; Creech, D.L.; Krauss, K.W.; Yunlong, Y.; Kulhavy, D.L. Can We Improve the Salinity Tolerance of Genotypes of *Taxodium* by Using Varietal and Hybrid Crosses? *Hortscience* **2010**, *45*, 1773–1778. [CrossRef]
38. Shi, Q.; Zhou, Z.D.; Wang, Z.Y.; Lu, Z.G.; Han, J.A.; Xue, J.H.; Creech, D.; Yin, Y.L.; Hua, J.F. Afforestation of *Taxodium* Hybrid Zhongshanshan Influences Soil Bacterial Community Structure by Altering Soil Properties in the Yangtze River Basin, China. *Plants* **2022**, *11*, 3456. [CrossRef] [PubMed]
39. Zeng, J.Y.; Ma, S.L.; Liu, J.; Qin, S.H.; Liu, X.; Li, T.; Liao, Y.; Shi, Y.X.; Zhang, J.C. Organic Materials and AMF Addition Promote Growth of *Taxodium* 'zhongshanshan' by Improving Soil Structure. *Forests* **2023**, *14*, 731. [CrossRef]
40. Tian, Y.; Dou, S.; Zhang, Y.; Wang, C.; Wu, J. Improvement effects of subsurface pipe with different spacing on sodic-alkali soil. *Editor. Off. Trans. Chin. Soc. Agric. Eng.* **2013**, *29*, 145–153.

41. Liu, X.; Cheng, X.F.; Wang, N.; Meng, M.J.; Jia, Z.H.; Wang, J.P.; Ma, S.L.; Tang, Y.Z.; Li, C.; Zhai, L.; et al. Effects of Vegetation Type on Soil Shear Strength in Fengyang Mountain Nature Reserve, China. *Forests* **2021**, *12*, 490. [CrossRef]

42. Cui, H.; Ma, K.; Fan, Y.; Peng, X.; Mao, J.; Zhou, D.; Zhang, Z.; Zhou, J. Stability and heavy metal distribution of soil aggregates affected by application of apatite, lime, and charcoal. *Environ. Sci. Pollut. Res. Int.* **2016**, *23*, 10808–10817. [CrossRef] [PubMed]

43. Setia, R.; Verma, S.L.; Marschner, P. Measuring microbial biomass carbon by direct extraction—Comparison with chloroform fumigation-extraction. *Eur. J. Soil Biol.* **2012**, *53*, 103–106. [CrossRef]

44. Zheng, X.; Liu, Q.; Cao, M.M.; Ji, X.F.; Lu, J.B.; He, L.; Liu, L.J.; Liu, S.L.; Jiang, J. Nitrogen uptake by plants may alleviate N deposition-induced increase in soil N₂O emissions in subtropical Chinese fir (*Cunninghamia lanceolata*) plantations. *Plant Soil* **2022**, *479*, 127–142. [CrossRef]

45. Stemmer, M.; Gerzabek, M.H.; Kandeler, E.J.S.B. Organic matter and enzyme activity in particle-size fractions of soils obtained after low-energy sonication. *Soil Biol. Biochem.* **1998**, *30*, 9–17. [CrossRef]

46. German, D.P.; Weintraub, M.N.; Grandy, A.S.; Lauber, C.L.; Rinkes, Z.L.; Allison, S.D. Optimization of hydrolytic and oxidative enzyme methods for ecosystem studies. *Soil Biol. Biochem.* **2012**, *43*, 1387–2011. [CrossRef]

47. Wang, L.; Jia, Z.Q.; Li, Q.X.; He, L.X.Z.; Tian, J.P.; Ding, W.; Liu, T.; Gao, Y.; Zhang, J.P.; Han, D.; et al. Grazing Impacts on Soil Enzyme Activities Vary with Vegetation Types in the Forest-Steppe Ecotone of Northeastern China. *Forests* **2023**, *14*, 2292. [CrossRef]

48. Li, C.; Jia, Z.H.; Peng, X.N.; Zhai, L.; Zhang, B.; Liu, X.; Zhang, J.C. Functions of mineral-solubilizing microbes and a water retaining agent for the remediation of abandoned mine sites. *Sci. Total Environ.* **2021**, *761*, 143215. [CrossRef] [PubMed]

49. Li, C.; Yu, Z.Z.; Lin, J.; Meng, M.J.; Zhao, Y.P.; Jia, Z.H.; Peng, X.N.; Liu, X.; Zhang, J.C. Forest Conversion and Soil Depth Can Modify the Contributions of Organic and Inorganic Colloids to the Stability of Soil Aggregates. *Forests* **2022**, *13*, 546. [CrossRef]

50. Na, L.; Tianyun, S.; Yujie, Z.; Yuchen, C.; Huiying, H.; Qingkai, S.; Xiaohua, L.; Yang, Y.; Xiumei, G.; Zed, R. Effects of planting *Melia azedarach* L. on soil properties and microbial community in saline-alkali soil. *Land Degrad. Dev.* **2021**, *32*, 2951–2961.

51. Xia, J.; Ren, J.; Zhang, S.; Wang, Y.; Fang, Y. Forest and grass composite patterns improve the soil quality in the coastal saline-alkali land of the Yellow River Delta, China. *Geoderma* **2019**, *349*, 25–35. [CrossRef]

52. Zhu, X.; Shen, Y.; Yuan, X.; Yuan, C.; Jin, L.; Zhao, Z.; Chen, F.; Yang, B.; Jiang, X.; Liu, W. High levels of soil calcium and clay facilitate the recovery and stability of organic carbon: Insights from different land uses in the karst of China. *Environ. Sci. Pollut. Res. Int.* **2024**, *31*, 34234–34248. [CrossRef] [PubMed]

53. Zhou, X.; Chen, X.; Yang, K.; Guo, X.; Liu, G.; Zhuang, G.; Zheng, G.; Fortin, D.; Ma, A. Vegetation restoration in an alpine meadow: Insights from soil microbial communities and resource limitation across soil depth. *J. Environ. Manag.* **2024**, *360*, 121129. [CrossRef]

54. Hu, P.L.; Xiao, J.; Zhang, W.; Xiao, L.M.; Yang, R.; Xiao, D.; Zhao, J.; Wang, K.L. Response of soil microbial communities to natural and managed vegetation restoration in a subtropical karst region. *Catena* **2020**, *195*, 104849. [CrossRef]

55. You, Y.; Li, W.; Chen, Y.; Zhang, Q.; Zhang, K. Soil carbon and nitrogen accumulation during long-term natural vegetation restoration following agricultural abandonment in Qingling Mountains. *Ecol. Eng.* **2024**, *201*, 107212. [CrossRef]

56. Song, W.T.; Hou, Y.K.; Zhu, W.J.; Fan, Y.C.; Xu, H.Y.; Cai, C.Y.; Li, G.H.; Huang, L. Enhancement effects of mangrove restoration on blue carbon storage in Qinzhou Bay. *Front. For. Glob. Change* **2024**, *7*, 1328783. [CrossRef]

57. Van Der Sande, M.T.; Powers, J.S.; Kuyper, T.W.; Norden, N.; Salgado-Negret, B.; Silva de Almeida, J.; Bongers, F.; Delgado, D.; Dent, D.H.; Derroire, G.; et al. Soil resistance and recovery during neotropical forest succession. *Philos. Trans. R. Soc. B* **2023**, *378*, 20210074. [CrossRef]

58. Deng, L.; Liu, G.B.; Shangguan, Z.P. Land-use conversion and changing soil carbon stocks in China's 'Grain-for-Green' Program: A synthesis. *Glob. Change Biol.* **2014**, *20*, 3544–3556. [CrossRef]

59. Karhu, K.; Wall, A.; Vanhala, P.; Liski, J.; Esala, M.; Regina, K. Effects of afforestation and deforestation on boreal soil carbon stocks—Comparison of measured C stocks with Yasso07 model results. *Geoderma* **2011**, *164*, 33–45. [CrossRef]

60. Zhang, K.; Dang, H.; Tan, S.; Cheng, X.; Zhang, Q. Change in soil organic carbon following the 'Grain-for-Green' programme in China. *Land Degrad. Dev.* **2009**, *21*, 13–23. [CrossRef]

61. Harper, R.J.; Tibbett, M. The hidden organic carbon in deep mineral soils. *Plant Soil* **2013**, *368*, 641–648. [CrossRef]

62. Fang, X.M.; Chen, F.S.; Wan, S.Z.; Yang, Q.P.; Shi, J.M. Topsoil and Deep Soil Organic Carbon Concentration and Stability Vary with Aggregate Size and Vegetation Type in Subtropical China. *PLoS ONE* **2015**, *10*, e0139380. [CrossRef]

63. Xie, M.; Yuan, J.; Liu, S.; Xu, G.; Lu, Y.; Yan, L.; Li, G. Soil Carbon and Nitrogen Pools and Their Storage Characteristics under Different Vegetation Restoration Types on the Loess Plateau of Longzhong, China. *Forests* **2024**, *15*, 173. [CrossRef]

64. Jiang, J.P.; Xiong, Y.C.; Jiang, H.M.; Ye, D.Y.; Song, Y.J.; Li, F.M. Soil Microbial Activity During Secondary Vegetation Succession in Semiarid Abandoned Lands of Loess Plateau. *Pedosphere* **2009**, *19*, 735–747. [CrossRef]

65. Lucas-Borja, M.E.; Hedo, J.; Cerdá, A.; Candel-Pérez, D.; Viñegla, B. Unravelling the importance of forest age stand and forest structure driving microbiological soil properties, enzymatic activities and soil nutrients content in Mediterranean Spanish black pine (*Pinus nigra* Ar. ssp. salzmannii) Forest. *Sci. Total Environ.* **2016**, *562*, 145–154. [CrossRef] [PubMed]

66. Kähkönen, M.A.; Hakulinen, R. Hydrolytic enzyme activities, carbon dioxide production and the growth of litter degrading fungi in different soil layers in a coniferous forest in Northern Finland. *Eur. J. Soil Biol.* **2011**, *47*, 108–113. [CrossRef]

67. Tang, L.L.; Wang, S.Q. Dynamics of soil aggregate-related C-N-P stoichiometric characteristics with stand age and soil depth in Chinese fir plantations. *Land Degrad. Dev.* **2022**, *33*, 1290–1306. [CrossRef]

68. Guan, Z.J.; Luo, Q.; Chen, X.; Feng, X.W.; Tang, Z.X.; Wei, W.; Zheng, Y.R. Saline soil enzyme activities of four plant communities in Sangong River basin of Xinjiang, China. *J. Arid. Land* **2014**, *6*, 164–173. [CrossRef]

69. Xiaodong, Y.; Wenjing, Z.; Hui, Z.; Wei, W. Soil Microbial Attributes along a Chronosequence of Scots Pine (*Pinus sylvestris* var. *mongolica*) Plantations in Northern China. *Pedosphere* **2017**, *30*, 433–442.

70. Kunito, T.; Akagi, Y.; Park, H.D.; Toda, H. Influences of nitrogen and phosphorus addition on polyphenol oxidase activity in a forested Andisol. *Eur. J. For. Res.* **2009**, *128*, 361–366. [CrossRef]

71. Feng, J.; Xu, X.; Wu, J.J.; Zhang, Q.; Zhang, D.D.; Li, Q.X.; Long, C.Y.; Chen, Q.; Chen, J.W.; Cheng, X.L. Inhibited enzyme activities in soil macroaggregates contribute to enhanced soil carbon sequestration under afforestation in central China. *Sci. Total Environ.* **2018**, *640*, 653–661. [CrossRef]

72. Yong-ling, W.; Bing, W.; Chao, Z.; Wei, D.; Li, P.; University, F. Comprehensive evaluation of soil fertility in different developing stages of Chinese Fir. *Plantations* **2011**, *39*, 69–75.

73. Wang, C.Q.; Xue, L.; Dong, Y.H.; Hou, L.Y.; Wei, Y.H.; Chen, J.Q.; Jiao, R.Z. Contrasting Effects of Chinese Fir Plantations of Different Stand Ages on Soil Enzyme Activities and Microbial Communities. *Forests* **2019**, *10*, 11. [CrossRef]

74. Zhao, F.Z.; Han, X.H.; Yang, G.H.; Feng, Y.Z.; Ren, G.X. Soil structure and carbon distribution in subsoil affected by vegetation restoration Plant Soil Environ. 2014, 64, 21–26. *64*.

75. Wei, X.R.; Li, X.Z.; Jia, X.X.; Shao, M.G. Accumulation of soil organic carbon in aggregates after afforestation on abandoned farmland. *Biol. Fertil. Soils* **2013**, *49*, 637–646. [CrossRef]

76. Wang, J.Y.; Deng, Y.S.; Li, D.Y.; Liu, Z.F.; Wen, L.L.; Huang, Z.G.; Jiang, D.H.; Lu, Y.P. Soil aggregate stability and its response to overland flow in successive *Eucalyptus* plantations in subtropical China. *Sci. Total Environ.* **2022**, *807*, 151000. [CrossRef] [PubMed]

77. Le Bissonnais, Y.; Prieto, I.; Roumet, C.; Nespoulous, J.; Metayer, J.; Huon, S.; Villatoro, M.; Stokes, A. Soil aggregate stability in Mediterranean and tropical agro-ecosystems: Effect of plant roots and soil characteristics. *Plant Soil* **2018**, *424*, 303–317. [CrossRef]

78. Laganière, J.; Angers, D.A.; PARÉ, D. Carbon accumulation in agricultural soils after afforestation: A meta-analysis. *Glob. Change Biol.* **2010**, *16*, 439–453. [CrossRef]

79. Zhang, Y.; Zhen, Q.; Ma, W.; Jia, J.; Li, P.; Zhang, X. Dynamic responses of soil aggregate-associated organic carbon and nitrogen to different vegetation restoration patterns in an agro-pastoral ecotone in northern China. *Ecol. Eng.* **2023**, *189*, 106895. [CrossRef]

80. Kurmi, B.; Nath, A.J.; Lal, R.; Das, A.K. Water stable aggregates and the associated active and recalcitrant carbon in soil under rubber plantation. *Sci. Total Environ.* **2020**, *703*, 135498. [CrossRef] [PubMed]

81. Zhao, M.Q.; Li, D.H.; Huang, Y.; Deng, Y.S.; Yang, G.R.; Lei, T.W.; Huang, Y.H. Soil matrix infiltration characteristics in differently aged eucalyptus plantations in a southern subtropical area in China. *Catena* **2022**, *217*, 106490. [CrossRef]

82. Yang, M.; Yang, D.; Yu, X. Soil microbial communities and enzyme activities in sea-buckthorn (*Hippophae rhamnoides*) plantation at different ages. *PLoS ONE* **2018**, *13*, e0190959. [CrossRef]

83. Erdel, E. Effects of Salinity and Alkalinity on Soil Enzyme Activities in Soil Aggregates of Different Sizes. *Eurasian Soil Sci.* **2022**, *55*, 759–765. [CrossRef]

84. Yang, Q.; Zhu, D.Y.; Chen, J. Effects of Planting Patterns on Soil Aggregates and Enzyme Activities in Rocky Desertification Areas of Karst Plateau Mountains. *Pol. J. Environ. Stud.* **2023**, *32*, 405–418. [CrossRef] [PubMed]

85. Haj-Amor, Z.; Araya, T.; Kim, D.G.; Bouri, S.; Lee, J.; Ghilou, W.; Yang, Y.; Kang, H.; Jhariya, M.K.; Banerjee, A.; et al. Soil salinity and its associated effects on soil microorganisms, greenhouse gas emissions, crop yield, biodiversity and desertification: A review. *Sci. Total Environ.* **2022**, *843*, 156946. [CrossRef] [PubMed]

86. Radersma, S.; Grierson, P.F. Phosphorus mobilization in agroforestry: Organic anions, phosphatase activity and phosphorus fractions in the rhizosphere. *Plant Soil* **2004**, *259*, 209–219. [CrossRef]

87. Zhang, D.B.; Yao, Z.Y.; Chen, J.; Yao, P.W.; Zhao, N.; He, W.X.; Li, Y.Y.; Zhang, S.Q.; Zhai, B.N.; Wang, Z.H.; et al. Improving soil aggregation, aggregate-associated C and N, and enzyme activities by green manure crops in the Loess Plateau of China. *Eur. J. Soil Sci.* **2019**, *70*, 1267–1279.